Immunity, Volume *53*

Supplemental Information

Multifaceted Effects of Antigen Valency on B Cell Response Composition and Differentiation *In Vivo*

Yu Kato, Robert K. Abbott, Brian L. Freeman, Sonya Haupt, Bettina Groschel, Murillo Silva, Sergey Menis, Darrell J. Irvine, William R. Schief, and Shane Crotty

Figure S1

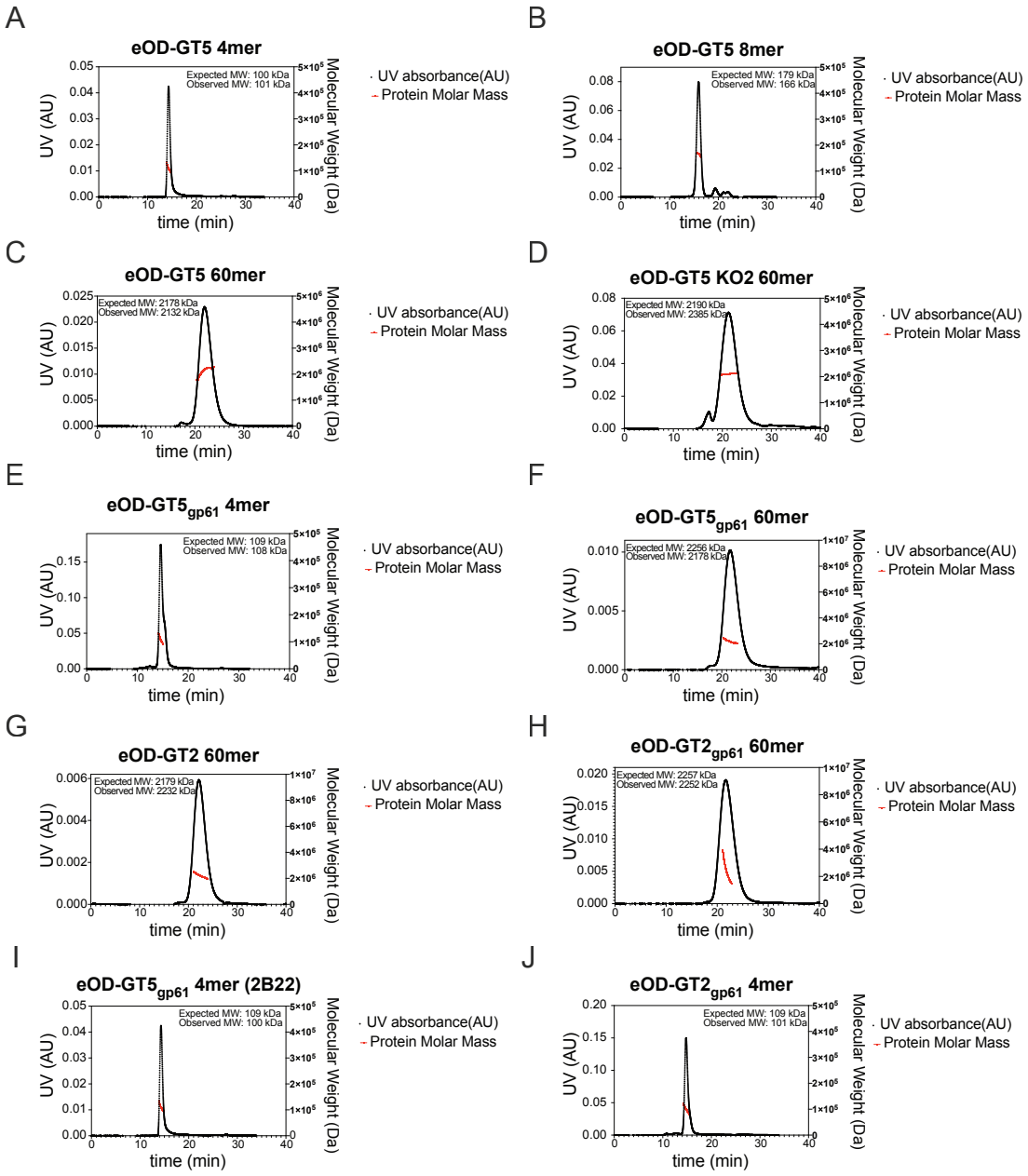

Figure S1. Characterization of recombinant protein multimers by size exclusion chromatography coupled in-line with a multi-angle light scattering detector (SEC-MALS), Related to Figure 1.

A–J, Traces show UV absorbance during the elution and lines under the peak the calculated protein molar mass of the eluting species.

(A) eOD-GT5 4mer. Calculated MW: 100 kDa, measured MW: 101 kDa.

(B) eOD-GT5 8mer. Calculated MW: 179 kDa, measured MW: 166 kDa.

(C) eOD-GT5 60mer. Calculated MW: 2178 kDa, measured MW: 2132 kDa.

(D) eOD-GT5-KO2 60mer. Calculated MW: 2190 kDa, measured MW: 2385 kDa.

(E) eOD-GT5$_{gp61}$ 4mer. Calculated MW: 109 kDa, measured MW: 108 kDa.

(F) eOD-GT5$_{gp61}$ 60mer. Calculated MW: 2256 kDa, measured MW: 2178 kDa.

(G) eOD-GT2 60mer. Calculated MW: 2179 kDa, measured MW: 2232 kDa.

(H) eOD-GT2$_{gp61}$ 60mer. Calculated MW: 2257 kDa, measured MW: 2252 kDa.

(I) eOD-GT5$_{gp61}$ 4mer (2B22). Calculated MW: 109 kDa, measured MW: 100 kDa.

(J) eOD-GT2$_{gp61}$ 4mer. Calculated MW: 109 kDa, measured MW: 101 kDa.

Figure S2

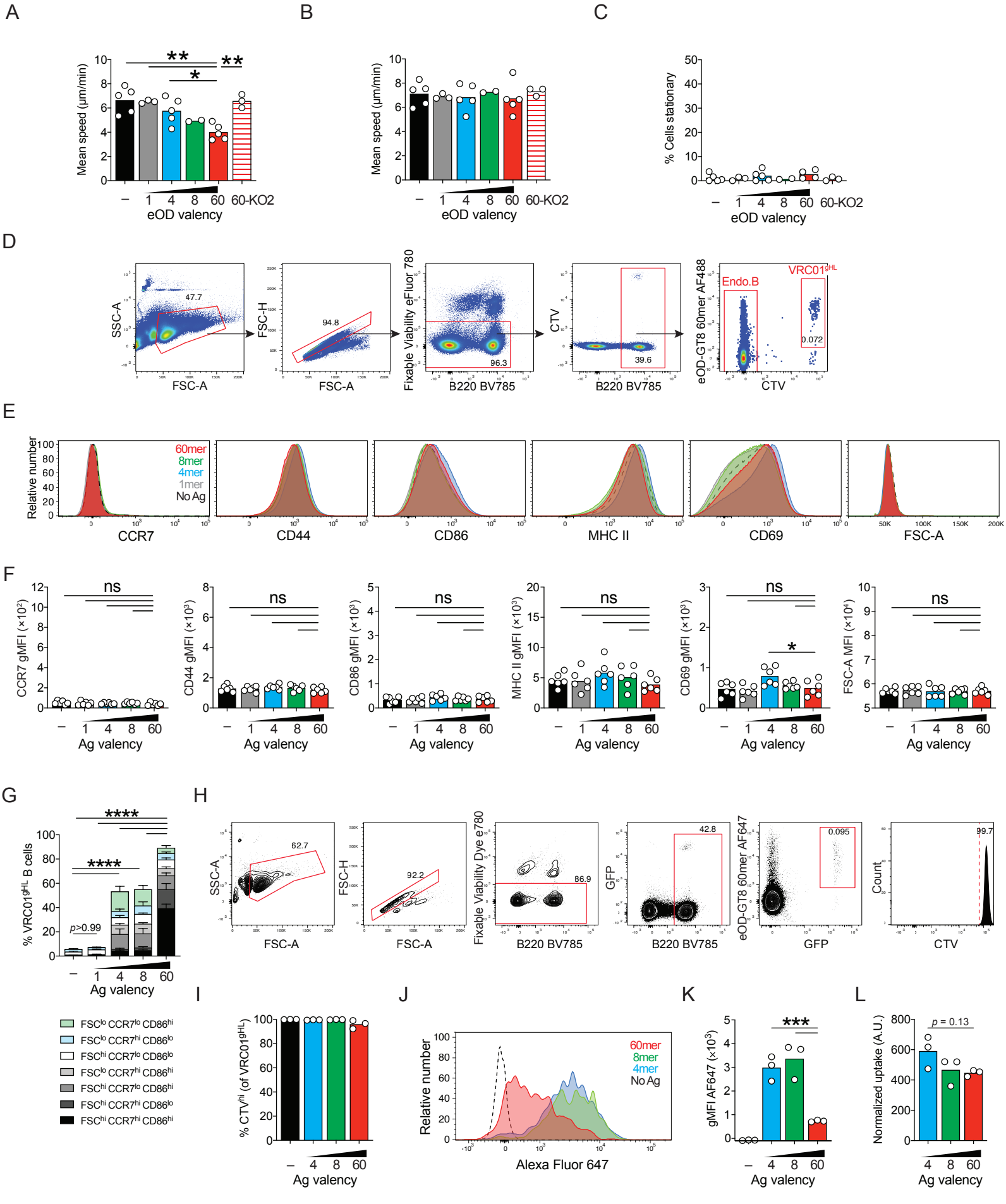
A
B
C
Mean speed (μm/min)
eOD valency
% Cells stationary
D
SSC-A
FSC-A
FSC-H
Fixable Viability eFluor 780
B220 BV785
CTV
eOD-GT8 60mer AF488
Endo.B
VRC01gHL
E
Relative number
60mer
8mer
4mer
1mer
No Ag
CCR7
CD44
CD86
MHC II
CD69
F
CCR7 gMFI (×10²)
CD44 gMFI (×10³)
CD86 gMFI (×10³)
MHC II gMFI (×10³)
CD69 gMFI (×10³)
FSC-A MFI (×10⁴)
ns
Ag valency
G
% VRC01gHL B cells
p>0.99
FSClo CCR7lo CD86hi
FSClo CCR7hi CD86lo
FSChi CCR7lo CD86lo
FSClo CCR7hi CD86hi
FSChi CCR7lo CD86hi
FSChi CCR7hi CD86lo
FSChi CCR7hi CD86hi
H
GFP
Count
I
% CTVhi (of VRC01gHL)
J
Alexa Fluor 647
K
gMFI AF647 (×10³)
L
Normalized uptake (A.U.)
p = 0.13

Figure S2. Protein antigens of quantitatively distinct valencies exhibit differential stimulation of cognate B cells *in vivo* within hours, Related to Figures 1 and 2.

A–C, Intravital two-photon imaging of draining inguinal LN was performed 2-3.5h after immunization with eOD-GT5 antigen constructs (1mer, 4mer, 8mer, or 60mer), eOD-GT5 KO 60mer, or PBS.

(A) Average migration speed of VRC01^{gHL} B cells (GFP$^+$ or CTV$^+$).

(B) Average migration speed of polyclonal B cells (CFP$^+$ or CTDR$^+$).

(C) Frequency of polyclonal B cells that were stationary (average speed less than 3μm/min).

Each point represents a mouse, n = 3 (1mer, KO 60mer), n = 5 (H, eOD-GT5 4mer, and 60mer), or n = 2 (eOD-GT5 8mer). Bars represent the mean.

(A-C) Pooled data from three adoptive transfer experiments. Statistical analysis (A–C) was performed by one-way ANOVA, followed by Tukey's test. *, $p < 0.05$; **, $p < 0.01$.

D–G, B6 mice adoptively transferred with 10^6 CTV$^+$ VRC01^{gHL} B cells were immunized with eOD-GT5 antigens and LNs were analyzed at 24h.

(D) Gating strategies to define VRC01^{gHL} B cells and endogenous B cells.

(E) Histograms showing endogenous B cell phenotype.

(F) Quantification of various surface molecules (geometric MFI) and FSC-A (mean).

(G) Multiple parameters (cell size, CCR7 and CD86) were examined in parallel to assess VRC01^{gHL} B cell activation. Mean percentage ± SEM.

(E-G) Pooled data from two independent experiments, $n = 6$ mice per group. Statistical analysis (F, G) was performed by one-way ANOVA, followed by Tukey's test. ns, $p > 0.05$; *, $p < 0.05$; ****, $p < 0.0001$.

H, **I**, B6 mice adoptively transferred with 10^6 CTV$^+$ GFP$^+$ VRC01^{gHL} B cells were immunized with eOD-GT5 antigens and LNs were analyzed at 24h.

(H) VRC01^{gHL} B cells were defined based as B220$^+$ GFP$^+$ eOD-binding live single lymphocytes. Plots shown are representative of mice immunized with 60mer. The CTV profile indicates lack of cell division at this time-point.

(I) Frequency of undivided cells of the total VRC01^{gHL} B cells at 24h based on CTV dilution.

(H, I) Data from one experiment, n = 3 mice per group.

J-L, B6 mice adoptively transferred with 10^6 CTV$^+$ VRC01^{gHL} B cells were immunized with eOD-GT5 4mer, 8mer or 60mer conjugated to Alexa Fluor 647. LNs were analyzed at 24h to quantify antigen uptake by VRC01^{gHL} B cells.

(J) Histograms gated on VRC01^{gHL} B cells showing Alexa Fluor 647 fluorescence.

(K) Quantification of geometric MFI of Alexa Fluor 647.

(L) Geometric MFI values were divided by the estimated numbers of Alexa Fluor 647 molecules conjugated per monomer (5.1 for 4mer, 7.3 for 8mer, 1.8 for 60mer).

(J-L) Data from one experiment, n = 3 mice per group. Statistical analysis (K, L) was performed by one-way ANOVA, followed by Tukey's test. ****, $p < 0.0001$.

Figure S3

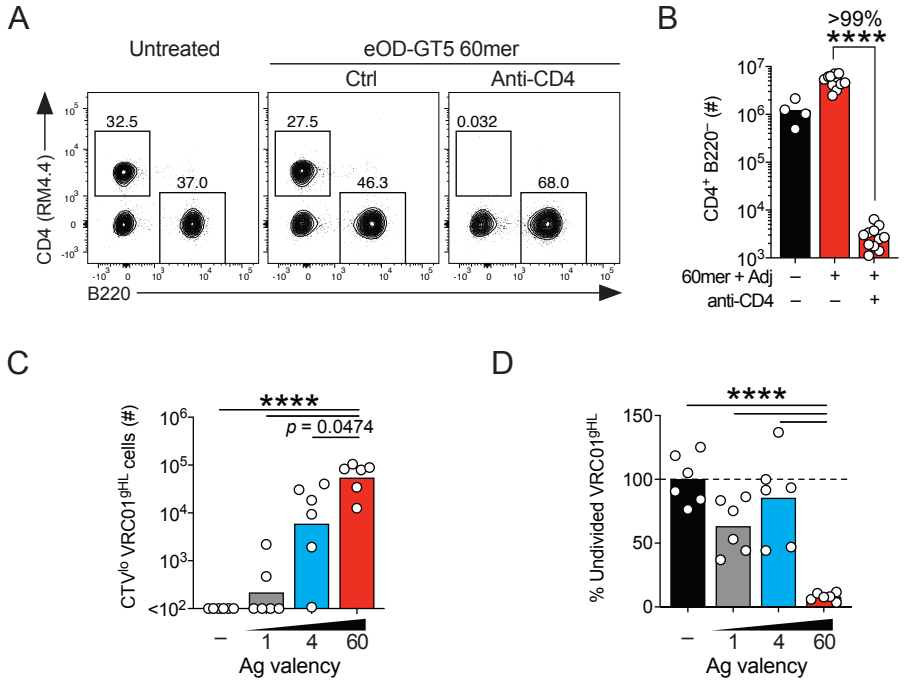

Figure S3. Low-valency antigens poorly induce B cell division, Related to Figure 3.

A, B, $CD4^+$ T cells were depleted using GK1.5 prior to vaccination with eOD-GT5 60mer. Efficiency of $CD4^+$ T cell depletion in iLN was assessed at d3 post-immunization.

(A) Representative FACS plots showing lymph node cells (gated as lymphocytes, singlets, live). The gates identify $CD4^+$ $B220^-$ T cells and $CD4^-$ $B220^+$ B cells. Number in each quadrant represents percentage.

(B) Quantification of $CD4^+$ $B220^-$ T cells in iLN at d3 post-immunization.

(A, B) Pooled data from four independent experiments, n = 6 (naive), n = 11 (60mer + Adj, isotype control), n = 10 (60mer + Adj, GK1.5). Statistical analysis (B) was performed on a log-transformed dataset by One-way ANOVA, followed by Tukey's test.

C, D, CTV^+ $VRC01^{gHL}$ B cells were adoptively transferred into B6 mice prior to vaccination with eOD-$GT5_{gp61}$ antigen constructs. $VRC01^{gHL}$ B cell proliferative responses were examined 7d after immunization..

(C) Divided $VRC01^{gHL}$ B cell numbers. Each point represents a mouse and bars represent the geometric mean.

(D) Normalized frequency of undivided $VRC01^{gHL}$ B cells in LN.

Pooled data from two independent experiments, n = 6 mice per group. Each point represents a mouse and bars represent the geometric mean (C) and arithmetic mean (D). Statistical analysis was performed using One-way ANOVA on log-transformed dataset (C) or untransformed dataset (D). ****, $p < 0.0001$

Figure S4

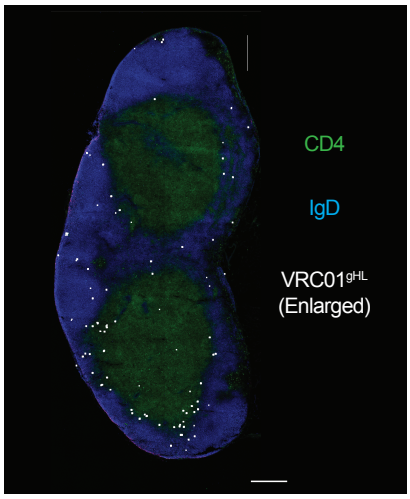

Figure S4. High-valency low-affinity antigen effectively induces early B cell responses, Related to Figure 4.

CTV^{+} VRC01^{gHL} B cells were adoptively transferred into B6 mice prior immunization with eOD-GT2 60m with adjuvant. Representative immunofluorescence images of frozen LN sections showing changes in the distribution of CTV^{+} VRC01^{gHL} B cells (white). IgD (blue) and CD4 (green) are visualized to highlight B cell zone and T cell zone, respectively. Individual VRC01^{gHL} B cell CTV signals were digitally dilated for enhanced visualization. Scale bar = 300μm.

Figure S5

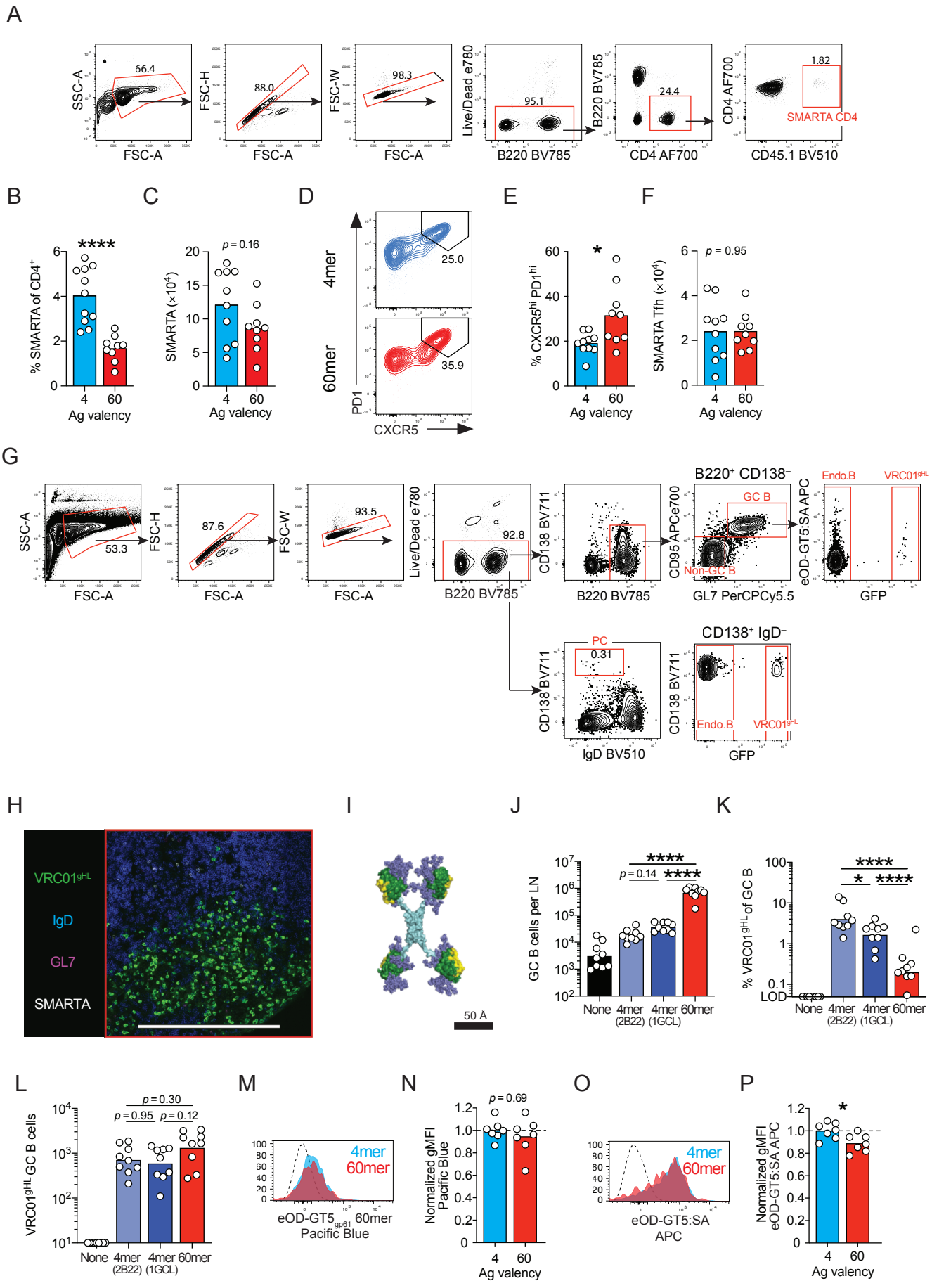
A
66.4
SSC-A
FSC-A
88.0
FSC-H
FSC-A
98.3
FSC-W
FSC-A
95.1
Live/Dead e780
B220 BV785
24.4
B220 BV785
CD4 AF700
1.82
SMARTA CD4
CD4 AF700
CD45.1 BV510
B
****
% SMARTA of CD4+
4
60
Ag valency
C
p = 0.16
SMARTA (×10⁴)
4
60
Ag valency
D
4mer
25.0
60mer
35.9
PD1
CXCR5
E
*
% CXCR5hi PD1hi
4
60
Ag valency
F
p = 0.95
SMARTA Tfh (×10⁴)
4
60
Ag valency
G
53.3
SSC-A
FSC-A
87.6
FSC-H
FSC-A
93.5
FSC-W
FSC-A
92.8
Live/Dead e780
B220 BV785
CD138 BV711
B220 BV785
B220+ CD138−
GC B
Non-GC B
CD95 APCe700
GL7 PerCPCy5.5
Endo.B
VRC01gHL
eOD-GT5:SA APC
GFP
PC
0.31
CD138 BV711
IgD BV510
CD138+ IgD−
CD138 BV711
Endo.B
VRC01gHL
GFP
H
VRC01gHL
IgD
GL7
SMARTA
I
50 Å
J
****
p = 0.14
****
GC B cells per LN
None
4mer (2B22)
4mer (1GCL)
60mer
K
****
*
****
% VRC01gHL of GC B
LOD
None
4mer (2B22)
4mer (1GCL)
60mer
L
p = 0.30
p = 0.95
p = 0.12
VRC01gHL GC B cells
None
4mer (2B22)
4mer (1GCL)
60mer
M
4mer
60mer
eOD-GT5gp61 60mer Pacific Blue
N
p = 0.69
Normalized gMFI Pacific Blue
4
60
Ag valency
O
4mer
60mer
eOD-GT5:SA APC
P
*
Normalized gMFI eOD-GT5:SA APC
4
60
Ag valency

Figure S5. High-valency antigen preferentially recruits low-affinity B cells into GCs, Related to Figures 5 and 6.

A-F, SMARTA $CD4^+$ T cell responses in iLNs were analyzed at d6 post-immunization with either eOD-$GT5_{gp61}$ 4mer or eOD-$GT5_{gp61}$ 60mer with adjuvant.

(A) Gating strategies to identify SMARTA $CD4^+$ T cells.

(B) Quantification of SMARTA $CD4^+$ T cell numbers. Each point represents a mouse. Bars indicate the mean.

(C) Quantification of SMARTA $CD4^+$ cells as a percentage of total $CD4^+$ T cells. Each point represents a mouse. Bars indicate the mean.

(D) Representative FACS plot of SMARTA $CD4^+$ T cells. The gate identifies $CXCR5^{hi}$ $PD1^{hi}$ T_{FH}. Number indicates the percentage.

(E) Frequency of SMARTA $CD4^+$ T cells that are $CXCR5^{hi}$ $PD1^{hi}$ T_{FH}. Each point represents a mouse. Bars indicate the mean.

(F) $CXCR5^{hi}$ $PD1^{hi}$ SMARTA T_{FH} cell numbers. Each point represents a mouse. Bars indicate the mean.

Data from three independent experiments. n = 10 mice (eOD-$GT5_{gp61}$ 4mer), n = 9 mice (eOD-$GT5_{gp61}$ 60mer). Statistical analysis (B–F) was performed using Mann-Whitney test. *, $p = 0.0220$; ****, $p < 0.0001$.

G, Gating strategies to define $GL7^-$ $CD95^-$ non-B_{GC}, $GL7^+$ $CD95^+$ B_{GC}, and IgD^- $CD138^+$ B_{PC}. $VRC01^{gHL}$ $B_{GC/PC}$ and endogenous (endo.) $B_{GC/PC}$ were distinguished based on GFP expression.

H, An example immunofluorescence image showing $VRC01^{gHL}$ B cells accumulating in the extrafollicular regions of iLN at d6 post-immunization with eOD-$GT5_{gp61}$ 60mer. $VRC01^{gHL}$ B cells (green), IgD (blue), GL7 (red), and SMARTA $CD4^+$ T cells (white). Scale bars = 300μm. Data representative of two-independent experiments, n = 6 mice.

I-K, GC responses in iLNs were analyzed at d6 post-immunization with adjuvant alone, or eOD-$GT5_{gp61}$ 4mer (2B22), eOD-$GT5_{gp61}$ 4mer (1GCL), or eOD-$GT5_{gp61}$ 60mer with adjuvant.

(I) Total B_{GC} number.

(J) Quantification of $VRC01^{gHL}$ B_{GC} as a percentage of total B_{GC}.

(K) Number of $VRC01^{gHL}$ B_{GC}.

(I–K) Data from three independent experiments. n = 9 mice (2B22, 1GCL, 60mer), n = 8 mice (adjuvant alone). Each point represents a mouse, bars indicate either the geometric mean.

L, To scale model of eOD-GT5 4mer (2B22) based on PDB ID 2B22. eOD is colored green, CD4 binding site is yellow, scaffold is cyan, and glycans are in slate. Proteins are shown in surface representation, and glycans are shown in sphere representation. Images were generated using PyMOL (The PyMOL Molecular Graphics System, Version 2.0 Schrödinger, LLC.).

M-P, Equivalent antigen-probes binding by $VRC01^{gHL}$ B cells *ex vivo* at d6 post-immunization with eOD-$GT5_{gp61}$ 4mer or 60mer.

(M) Representative histogram showing eOD-$GT5_{gp61}$ 60mer Pacific Blue probe binding.

(N) Quantification of eOD-$GT5_{gp61}$ 60mer probe binding (geometric MFI) normalized to 4mer group.

(O) Representative histogram showing eOD-GT5 monomer probe binding.

(P) Quantification of eOD-GT5 monomer probe binding (geometric MFI) normalized to 4mer group.

(M-P) Data from two independent experiments, n = 7 mice. Each point represents a mouse, bars represent the mean. Statistical analysis was performed by Mann-Whitney U test. *, $p = 0.0262$. ****, $p < 0.0001$.

Figure S6

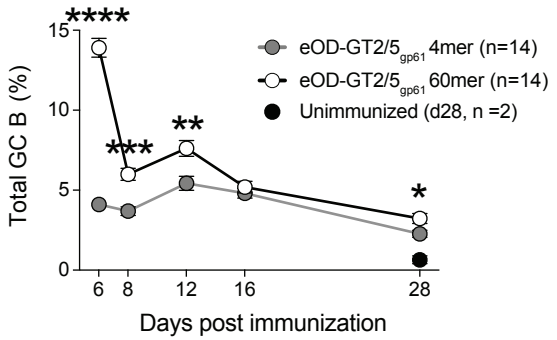

Figure S6. High-valency antigen induces strong GC responses. Related to Figure 7.
Quantification of B_{GC} as a percentage of total B cells over the course of 28d after immunization with eOD-GT2/5_{gp} 4mers or eOD-GT2/5_{gp} 60mers. Statistical analysis was performed by Mann-Whitney U test. *, $p < 0.05$; **, $p < 0.01$; **, $p < 0.001$; ****, $p < 0.0001$.

eOD construct	Amino acid sequence
eOD-GT2$_{gp61}$ 60mer	TGMQIYEGKLTAEGLRFGIVASRANHALVDRLVEGAIDAIVRHGGREEDITLVRVCGSWEIPVAAGELARKEDIDAVIAIGVLCRGAT PSFDYIASEVSKGLADLSLELRKPITFGVITADTLEQAIEAAGTCHGNKGWEAALCAIEMANLFKSLRGLKGPDIYKGVYQFKSVEFD DTITLPCRPAPPPHCSSNITGLILTRGGGISDDKTEIFRPGGGDMRDIARCQIAGTVVSTQLLLNGSLAEEEVVIRSEDFRDNSKSICV QLNTSVEINCTGAGHCNISRAKWNNTLKQIASKLREQFGNKTIIFSQSLGGDPEFVTHSFNCGGEFFYCDSTQLFDSTWFDS
eOD-GT5$_{gp61}$ 60mer	TGMQIYEGKLTAEGLRFGIVASRANHALVDRLVEGAIDAIVRHGGREEDITLVRVCGSWEIPVAAGELARKEDIDAVIAIGVLCRGAT PSFDYIASEVSKGLADLSLELRKPITFGVITADTLEQAIEAAGTCHGNKGWEAALCAIEMANLFKSLRGLKGPDIYKGVYQFKSVEFD DTITLPCRPAPPPHCSSNITGLILTRGGGVSDDDTEIFRPSGGDMRDIARCQIAGTVVSTQLFLNGSLAEEEVVIRSVDFRDNAKSICV QLNTSVEINCTGAGHCNISRAKWNNTLKQIASKLREQFGNRTIIFSQSSGGDPEFVTHSFNCGGEFFYCDSTQLFDSTWFDST
eOD-GT2$_{gp61}$ 4mer	TGDTITLPCRPAPPPHCSSNITGLILTRGGGISDDKTEIFRPGGGDMRDIARCQIAGTVVSTQLLLNGSLAEEEVVIRSEDFRDNSKSIC VQLNTSVEINCTGAGHCNISRAKWNNTLKQIASKLREQFGNKTIIFSQSLGGDPEFVTHSFNCGGEFFYCDSTQLFDSTWFDSTGS GGSGGSGGSGGSGGSGRMKQIEDKLEEILSKLYHIENELARIKKLLGERGTKHHHHHHGLKGPDIYKGVYQFKSVEFD
eOD-GT5$_{gp61}$ 4mer	TGDTITLPCRPAPPPHCSSNITGLILTRGGGVSDDDTEIFRPSGGDMRDIARCQIAGTVVSTQLFLNGSLAEEEVVIRSVDFRDNAKSI CVQLNTSVEINCTGAGHCNISRAKWNNTLKQIASKLREQFGNRTIIFSQSSGGDPEFVTHSFNCGGEFFYCDSTQLFDSTWFDST GSGGSGGSGGSGGSGRMKQIEDKLEEILSKLYHIENELARIKKLLGERGTKHHHHHHGLKGPDIYKGVYQFKSVEFD
eOD-GT5$_{gp61}$ 4mer (2B22)	TGDTITLPCRPAPPPHCSSNITGLILTRGGGVSDDDTEIFRPSGGDMRDIARCQIAGTVVSTQLFLNGSLAEEEVVIRSVDFRDNAKSI CVQLNTSVEINCTGAGHCNISRAKWNNTLKQIASKLREQFGNRTIIFSQSSGGDPEFVTHSFNCGGEFFYCDSTQLFDSTWFDST GSGGSGGSGGSGGSGMKVKQLEDVVEELLSVNYHLENVVARLKKLVGERGTKHHHHHHGLKGPDIYKGVYQFKSVEF
eOD-GT5 4mer	TGDTITLPCRPAPPPHCSSNITGLILTRGGGVSDDDTEIFRPSGGDMRDIARCQIAGTVVSTQLFLNGSLAEEEVVIRSVDFRDNAKSI CVQLNTSVEINCTGAGHCNISRAKWNNTLKQIASKLREQFGNRTIIFSQSSGGDPEFVTHSFNCGGEFFYCDSTQLFDSTWFDST GSGGSGGSGGSGGSGRMKQIEDKLEEILSKLYHIENELARIKKLLGERGTKHHHHHH
eOD-GT5 8mer	TGDTITLPCRPAPPPHCSSNITGLILTRGGGVSDDDTEIFRPSGGDMRDIARCQIAGTVVSTQLFLNGSLAEEEVVIRSVDFRDNAKSI CVQLNTSVEINCTGAGHCNISRAKWNNTLKQIASKLREQFGNRTIIFSQSSGGDPEFVTHSFNCGGEFFYCDSTQLFDSTWFDST GSGGSGGSGGSGGSGMKVKQLEDVVEELLSVNYHLENVVARLKKLVGERGSGGSGGSGGSGGSGDTITLPCRPAPPPHCSSNIT GLILTRGGGVSDDDTEIFRPSGGDMRDIARCQIAGTVVSTQLFLNGSLAEEEVVIRSVDFRDNAKSICVQLNTSVEINCTGAGHCNIS RAKWNNTLKQIASKLREQFGNRTIIFSQSSGGDPEFVTHSFNCGGEFFYCDSTQLFDSTWFDSTGTKHHHHHH
eOD-GT2 60mer	TGMQIYEGKLTAEGLRFGIVASRANHALVDRLVEGAIDAIVRHGGREEDITLVRVCGSWEIPVAAGELARKEDIDAVIAIGVLCRGAT PSFDYIASEVSKGLADLSLELRKPITFGVITADTLEQAIEAAGTCHGNKGWEAALCAIEMANLFKSLRGGSGGSGGSGGSGGSGGDTI TLPCRPAPPPHCSSNITGLILTRGGGISDDKTEIFRPGGGDMRDIARCQIAGTVVSTQLLLNGSLAEEEVVIRSEDFRDNSKSICVQLN TSVEINCTGAGHCNISRAKWNNTLKQIASKLREQFGNKTIIFSQSLGGDPEFVTHSFNCGGEFFYCDSTQLFDSTWFDST
eOD-GT5 60mer	TGMQIYEGKLTAEGLRFGIVASRANHALVDRLVEGAIDAIVRHGGREEDITLVRVCGSWEIPVAAGELARKEDIDAVIAIGVLCRGAT PSFDYIASEVSKGLADLSLELRKPITFGVITADTLEQAIEAAGTCHGNKGWEAALCAIEMANLFKSLRGGSGGSGGSGGSGGSGGDTI TLPCRPAPPPHCSSNITGLILTRGGGVSDDDTEIFRPSGGDMRDIARCQIAGTVVSTQLFLNGSLAEEEVVIRSVDFRDNAKSICVQL NTSVEINCTGAGHCNISRAKWNNTLKQIASKLREQFGNRTIIFSQSSGGDPEFVTHSFNCGGEFFYCDSTQLFDSTWFDST
eOD-GT5-KO2 60mer	TGMQIYEGKLTAEGLRFGIVASRFNHALVDRLVEGAIDAIVRHGGREEDITLVRVPGSWEIPVAAGELARKEDIDAVIAIGVLIRGATP HFDYIASEVSKGLADLSLELRKPITFGVITADTLEQAIERAGTKHGNKGWEAALSAIEMANLFKSLRGGSGGSGGSGGSGGSGGDTITL PCRPAPPPHCSSNITGLILTRGGGVSDDDTEIFRPSGGDMRDIARCQIAGTVVSTQLFLNGSLAEEEVVIRSVDFRD**R**AKSICVQLNT SVEINCTGAGHCNISRAKWNNTLKQIASKLREQFGNRTIIFSQS**L**GG**R**PE**R**VTHSFNCGGEFFYCDSTQLFDSTWFDST
Avi-tagged eOD-GT5	TGDTITLPCRPAPPPHCSSNITGLILTRGGGVSDDDTEIFRPSGGDMRDIARCQIAGTVVSTQLFLNGSLAEEEVVIRSVDFRDNAKSI CVQLNTSVEINCTGAGHCNISRAKWNNTLKQIASKLREQFGNRTIIFSQSSGGDPEFVTHSFNCGGEFFYCDSTQLFDSTWFDST GTKHHHHHHGGSGGSGLNDIFEAQKIEWHE
Avi-tagged eOD-GT2	TGDTITLPCRPAPPPHCSSNITGLILTRGGGISDDKTEIFRPGGGDMRDIARCQIAGTVVSTQLLLNGSLAEEEVVIRSEDFRDNSKSIC VQLNTSVEINCTGAGHCNISRAKWNNTLKQIASKLREQFGNKTIIFSQSLGGDPEFVTHSFNCGGEFFYCDSTQLFDSTWFDSTGT KHHHHHHGGSGGSGLNDIFEAQKIEWHE
Avi-tagged eOD-GT5-KO2	TGDTITLPCRPAPPPHCSSNITGLILTRGGGVSDDDTEIFRPSGGDMRDIARCQIAGTVVSTQLFLNGSLAEEEVVIRSVDFRD**R**AKSI CVQLNTSVEINCTGAGHCNISRAKWNNTLKQIASKLREQFGNRTIIFSQS**L**GG**R**PE**R**VTHSFNCGGEFFYCDSTQLFDSTWFDST GTKHHHHHHGGSGGSGLNDIFEAQKIEWHE

Table S1. Amino acid sequences of eOD constructs, Related to Figure 1 and STAR Methods.
eOD-GT2 is indicated in blue, eOD-GT5 is indicated in red. LCMV gp$_{61-80}$ is underlined. Mutations in the CD4 binding site are indicated in bold.